Abstract

Co-contamination with chlorinated compounds and 1,4-dioxane has been reported at many sites. Recently, there has been an increased interest in bioremediation because of the potential to degrade multiple contaminants concurrently. Towards improving bioremediation efficacy, the current study examined laboratory microcosms (inoculated separately with two soils) to determine the phylotypes and functional genes associated with the biodegradation of two common co-contaminants (*cis*-dichloroethene [cDCE] and 1,4-dioxane). The impact of amending microcosms with lactate on cDCE and 1,4-dioxane biodegradation was also investigated. The presence of either lactate or cDCE did not impact 1,4-dioxane biodegradation one of the two soils. Lactate appeared to improve the initiation of the biological removal of cDCE in microcosms inoculated with either soil. Stable isotope probing (SIP) was then used to determine which phylotypes were actively involved in carbon uptake from cDCE and 1,4-dioxane in both soil communities. The most enriched phylotypes for ^{13}C assimilation from 1,4-dioxane included *Rhodopseudomonas* and *Rhodanobacter*. Propane monooxygenase was predicted (by PICRUSt2) to be dominant in the 1,4-dioxane amended microbial communities and propane monooxygenase gene abundance values correlated with other enriched (but less abundant) phylotypes for ^{13}C-1,4-dioxane assimilation. The dominant enriched phylotypes for ^{13}C assimilation from cDCE included *Bacteriovorax*, *Pseudomonas* and *Sphingomonas*. In the cDCE amended soil microcosms, PICRUSt2 predicted the presence of DNA encoding glutathione S-transferase (a known cDCE upregulated enzyme). Overall, the work demonstrated concurrent removal of cDCE and 1,4-dioxane by indigenous soil microbial communities and the enhancement of cDCE removal by lactate. The data generated on the phylotypes responsible for carbon uptake (as determined by SIP) could be incorporated into diagnostic molecular methods for site characterization. The results suggest concurrent biodegradation of cDCE and 1,4-dioxane should be considered for chlorinated solvent site remediation.

1. Introduction

The clean-up of sites with mixed contamination poses a significant challenge to the remediation community. Developing synergistic approaches that could reduce the concentrations of multiple contaminants has the potential to result in considerable cost savings. From the list of co-

contaminants found in soil and groundwater, the chlorinated solvents and their metabolites (tetrachloroethene [PCE], trichloroethene [TCE], *cis*-dichloroethene [cDCE], vinyl chloride [VC]) are particularly prevalent (found at > 3,000 Department of Defense sites) and problematic due to their tendency to form large, dissolved-phase plumes, their recalcitrant nature and the subsequent risk to human health. Remediation efforts have frequently involved biostimulation, through the addition of carbon sources, or bioaugmentation, through the injection of mixed microbial cultures containing *Dehalococcoides mccartyi* (Steffan and Vainberg, 2013). Although clearly a very successful approach, bioremediation with *D. mccartyi* involves several significant limitations and thus may not be appropriate for all chlorinated solvent contaminated sites. Specifically, it is unlikely to be employed at large oxic sites because of the requirement for highly reducing conditions for *D. mccartyi* and the associated cost of driving such large sites anaerobic. Secondly, the approach will be less desirable at sites with multiple contaminants if those co-contaminants can be degraded more easily under aerobic conditions (e.g. benzene, toluene, 1,4-dioxane). Further, the accumulation of the known human carcinogen, VC, from the dechlorination process represents a significant risk if complete dechlorination does not occur. Additionally, driving sites anaerobic can result in long-term secondary groundwater impacts such as hydrogen sulfide formation, acidification, mobilization of reduced metals and methane accumulation. In contrast, aerobic approaches have the advantage that the geochemistry of the site is not significantly impacted.

cDCE is a major degradation product of TCE by both abiotic and biotic degradation (Brown et al., 2009). In fact, “cDCE stall” is a well-recognized term in the remediation community for the accumulation of cDCE at chlorinated solvent sites. Given the common occurrence of cDCE, identifying the potential for cDCE transformation remains an important issue. 1,4-Dioxane, a probable human carcinogen and common chlorinated solvent stabilizer, has been found at numerous contaminated sites across the U.S. (EPA, 2017; Zenker et al., 2003). In an examination from 49 remediation installations at U.S. Air Force sites, 1,4-dioxane was detected in 781 groundwater wells, with the percentage of 1,4-dioxane with TCE in all 1,4- dioxane detection-positive wells being 64.4% (Anderson et al., 2012). In an evaluation of >2000 sites in California, the chlorinated solvents were found in 94% of the sites with detections of 1,4-dioxane (Adamson et al., 2014).

To address the problem of co-contamination, efforts have focused specifically on the removal of both chlorinated compounds and 1,4-dioxane. To degrade TCE, DCEs with 1,4-dioxane, *P. dioxanivorans* CB1190 was combined hydrogen peroxide and tungstated zirconia, which partially removed those contaminants with the remainder being degraded by *P. dioxanivorans* CB1190 (Miao et al., 2019; Miao et al., 2020). In another study, *P. dioxanivorans* CB1190 was combined with the anaerobic bioaugmentation culture KB-1 (a chloroethene degrading consortium) resulting in TCE transformation to cDCE, as well as cDCE and 1,4-dioxane degradation by *P. dioxanivorans* CB1190 (Polasko et al., 2019). Another strain *Azoarcus* sp. DD4, was found to degrade 1,4-dioxane with 1,1-DCE using propane as the main substrate (Deng et al., 2018). More recently, *Azoarcus* sp. DD4 was sequentially used with SDC-9 (another chloroethene degrading consortium) to achieve transformation of TCE to cDCE and VC by SDC-9 and co-metabolic removal of VC, cDCE and 1,4-dioxane by *Azoarcus* sp. DD4 with the addition of propane (Li et al., 2021). These studies suggest mixed microbial communities will likely be needed to facilitate co-contamination remediation. An interesting question arising from these trends concerns the biodegrading abilities of indigenous mixed communities and their potential contribution to site remediation.

Towards understanding the potential of natural mixed communities, the current work builds on previous research documenting aerobic 1,4-dioxane biodegradation in soil microcosms (Ramalingam and Cupples, 2020). In the current work, stable isotope probing (SIP) is utilized to identify which microorganisms are involved in carbon uptake from cDCE and 1,4-dioxane. SIP is a cultivation independent method to link identity with function (Radajewski et al., 2000) such as contaminant biodegradation (Aoyagi et al., 2018; Cho et al., 2013; Jayamani and Cupples, 2015; Paes et al., 2015; Sun et al., 2012). As aerobic contaminant biodegradation often relies on co-metabolism, the impact of an additional substrate (lactate) was also investigated. Lactate was selected because it is commonly used in biostimulation (to drive sites anaerobic) (Ellis et al., 2000; Fennell et al., 2001) and would therefore already be acceptable to many regulatory agencies. The objectives were to 1) examine removal rates of the co-contaminants cDCE and 1,4-dioxane, with and without lactate addition, with indigenous mixed microbial communities 2) identify the microorganisms responsible for the uptake of ^{13}C from cDCE as well as from 1,4-dioxane during biodegradation and 3) predict the functional genes present and correlate their

presence to specific phylotypes. The overall rationale behind the current project is to provide knowledge to enhance the remediation of two important groundwater contaminants (cDCE, 1,4-dioxane).

2. Methods

2.1 Chemicals and soil inocula

Unlabeled 1,4-dioxane (99.8%) and cDCE were purchased from Sigma-Aldrich (MO, USA). Labeled 1,4-dioxane [$(^{13}C)_4H_8O_2$] was purchased from Santa Cruz Biotechnology (TX, USA) with 99.2% isotopic purity and 98% purity, and labeled cDCE [$^{13}C_2H_2Cl_2$] was purchased from Sigma-Aldrich (MO, USA) with 99% isotopic purity and 97% purity. Two soils were collected from 5 sampling stations in 6 replicate plots within Treatments 1 and 2 at the Michigan State University (MSU) Main Cropping System Experiment at Kellogg Biological Station Long-Term Ecological Research (KBS LTER) (42°24′N, 85°23′W). Both soils received conventional levels of chemical inputs, however, Treatment 1 is chisel plowed and Treatment 2 is under no-till management. For additional information see https://lter-kbs-msu-edu.proxy1.cl.msu.edu/research/site-description-and-maps/. All samples for each treatment were mixed, then stored at 4 °C in the dark. These soils were selected because the analysis of shotgun sequencing data generated from a previous study (Thelusmond et al., 2019) indicated the presence of numerous microorganisms previously associated with 1,4-dioxane and cDCE biodegradation (as discussed in the results section).

2.2 Microcosms setup

For each set of amendments, microcosms were established in 160 mL serum bottles (wrapped with aluminum foil) with 10 g of soil and 20 mL of media. For each soil, triplicate microcosms were amended with one of the following four sets of amendments: 1) cDCE, 1,4-dioxane and lactate, 2) cDCE and 1,4-dioxane, without lactate, 3) 1,4-dioxane with lactate and 4) cDCE with lactate. All microcosms were closed with a rubber seal and aluminum crimp. For each soil, all four treatments included triplicate abiotic autoclaved controls. All bottles were incubated at room temperature (~21 °C) on a shaker (110 rpm). The media was based on that used to enrich the 1,4-dioxane degrader *Pseudonocardia dioxanivorans* CB1190 (except nitrilotriacetic acid was removed) (Parales et al., 1994). One liter of the media contained 100 mL of a buffer stock

[K_2HPO_4 (32.4 g/L), KH_2PO_4 (10 g/L), NH_4Cl (20 g/L)] and 100 mL of a trace metal stock [$MgSO_4.7H_2O$ (2 g/L), $FeSO_4.7H_2O$ (0.12 g/L), $MnSO_4.H_2O$ (0.03 g/L), $ZnSO_4.7H_2O$ (0.03 g/L), and $CoCl_2.6H_2O$ (0.01 g/L)]. The initial liquid concentrations of 1,4-dioxane and cDCE were ~ 6 mg/L and ~ 4 mg/L. The liquid concentration of cDCE was calculated based on Henry's law (Gossett, 1987). The treatments with sodium lactate were amended at 0.56 g/L (~5 mM).

Additional microcosms were established for each soil (160 mL bottles, 10 g soil 1 or 2, same media) for the SIP experiments. For each soil, triplicate abiotic control microcosms (sterilized by autoclaving) and six microcosms were amended with unlabeled 1,4-dioxane or cDCE (similar concentrations as above). Another six microcosms were amended with ^{13}C labeled 1,4-dioxane or ^{13}C labeled cDCE. As the above experiments indicated cDCE was improved by the addition of lactate, the cDCE bottles were also amended with 5 mM of lactate (and closed with a rubber seal and aluminum crimp). Although the microcosms amended with cDCE were initially aerobic, the final electron accepting conditions of these microcosms were not determined. The 1,4-dioxane amended bottles were not amended with lactate and were opened for 6 hours every three days for aeration.

2.3 Analytical methods

Liquid samples (0.1 mL) were withdrawn (with sterilized disposal needles and a 1 mL syringe), then filtered (with a 0.22 μm, 4 mm nylon syringe filter, Thomas Scientific, NJ) for 1,4-dioxane analysis. The filtered samples were injected into a GC-FID (Hewlett Packard 5890) equipped with a column (Restek, Stabilwax-DB, 30m, 0.53 mmID, 1μm) using a similar method to that previously described (Myers et al., 2018). The injector temperature was maintained at 220 °C and the detector temperature was set at 250 °C. The oven temperature was programmed to initiate at 80 °C for 1 min, then increased to 140 °C with a ramp of 20 °C /min. The gas phase concentration of cDCE was determined (1 mL gastight syringe, 0.2 mL of the gaseous sample) with a GC-FID (Hewlett Packard 5890) equipped with a capillary column (Alltech, AT-624, 30m × 0.53mm ID × 3.0μm) using a similar method described in a previous study (Freedman and Gossett, 1989). The injector temperature was maintained at 180 °C and the detector at 240 °C. The oven temperature was programmed to initiate at 45 °C for 4 min, then increased to 165 °C with a ramp of 20 °C /min, held at 165 °C for 1 min.

2.4 DNA extraction, fractionation and sequencing

Duplicate soil 1 and soil 2 inoculated microcosms amended with either labeled or unlabeled chemicals (16 bottles, 2 chemicals, 2 with unlabeled amendment X 2 with labeled amendment X 2 soils) were sacrificed for DNA extraction at ~50% cDCE or 1,4-dioxane removal using QIAGEN PowerSoil DNA extraction kit as per manufacturer's protocol. DNA extracts (approx. 10 µg) were loaded into Quick-Seal polyallomer tubes (13 by 51 mm, 5.1 mL; Beckman Coulter (Brea, CA) along with a Tris-EDTA (10 mM Tris, 1 mM EDTA, pH 8)-CsCl solution for ultracentrifugation. The density of the mixture inside the tube was determined with a model AR200 digital refractometer (Leica Microsystems Inc., Buffalo Grove, IL), and it was adjusted to a final value of 1.730 g/mL by adding small volumes of CsCl solution or TE buffer until the tube could be sealed. The sealed tubes were then ultracentrifuged at 178,000×g (20 °C) for 46 h in a StepSaver 70 V6 vertical titanium rotor (8 by 5.1 mL capacity) within a Sorvall WX 80 Ultra Series centrifuge (Thermo Scientific, Waltham, MA). Following ultracentrifugation, the tubes were placed onto a fraction system (Beckman Coulter) and fractions (~26, 200 µL) were collected. The buoyant density of each fraction was measured, and CsCl was removed by glycogen-assisted ethanol precipitation. The DNA concentration in each fraction was quantified using the Quant-iT™ dsDNA High-Sensitivity Assay Kit.

For each chemical (labeled and unlabeled) and soil, triplicate DNA extracts of three fractions with higher buoyant density (1.73-1.75 g/mL) and one fraction with lighter buoyant density (~1.70 g/mL) were submitted for 16S rRNA gene amplicon sequencing at Research Technology Support Facility (RTSF) at MSU. The heavy buoyant density fractions were selected based on the minimum concentration of DNA required for sequencing. In total, two 96 well plates were submitted for sequencing (2 chemicals, 2 soils, 4 fractions, 3 replicate fractions, 2 microcosm replicates, 2 isotopes). The V4 hypervariable region of the 16S rRNA gene was amplified using dual indexed Illumina compatible primers 515f/806r as described by Kozich, JJ (2013) (Kozich et al., 2013). PCR products were batch normalized using Invitrogen SequalPrep DNA Normalization plates and the products recovered from the plates pooled. The pool was cleaned up and concentrated using AmpureXP magnetic beads; it was QC'd and quantified using a combination of Qubit dsDNA HS, Agilent 4200 TapeStation HS DNA1000 and Kapa Illumina

Library Quantification qPCR assays. The pool was loaded onto an Illumina MiSeq v2 standard flow cell and sequencing was performed in a 2x250 bp paired end format using a MiSeq v2 500 cycle reagent cartridge. Custom sequencing and index primers were added to appropriate wells of the reagent cartridge. Base calling was performed by Illumina Real Time Analysis (RTA) v1.18.54 and output of RTA was demultiplexed and converted to FastQ format with Illumina Bcl2fastq v2.19.1. The sequencing data for 1,4-dioxane and cDCE SIP was submitted to NCBI under Bioproject PRJNA719874 (accession numbers SAMN18623434 to SAMN18623529) and PRJNA719920 (accession numbers SAMN18624005 to SAMN18624100), respectively.

2.5 Analysis of sequencing data

The amplicon sequencing data in the fastq file format was analyzed with Mothur (version 1.44.2) (Schloss, 2009) using the MiSeq Standard Operating Procedure (Kozich et al., 2013). The procedure included trimming the raw sequences and quality control. The database used for alignment was SILVA bacteria database (Release 138) for the V4 region (Pruesse et al., 2007). Chimeras, mitochondrial and chloroplast lineage sequences were removed, then the sequences were classified into OTUs. The downstream analysis was conducted using microbiome (Lahti and Shetty, 2017) (version 1.10.0), phyloseq (McMurdie and Holmes, 2013) (version 1.32.0), ampvis2 (Andersen et al., 2018) (version 2.6.5), ggplot2 (Wickham, 2016) (version 3.3.2), Hmisc (Harrell, 2020) (version 4.4-1), Matrix (Bates et al., 2019) (version 1.2-18), igraph (Csardi and Nepusz, 2006) (version 1.2.6), ggpubr (Kassambara, 2020) (version 0.4.0), vegan (Oksanen et al., 2020) (version 2.5-7) in R (R Core Team, 2018) (version 4.0.4) with R studio (RStudio Team, 2020) (version 1.1.456). Additionally, the software Statistical Analysis of Taxonomic and Functional Profiles (STAMP) (Parks et al., 2014) (version 2.1.3) was utilized to statistically analyze the results.

The package microbiome was used to combine the OTUs shared file, taxonomy and metadata and it was also used to transform the counts of reads for OTUs into relative abundance. Phyloseq and ggplot2 were used for the Non-metric Multi-dimensional Scaling (NMDS) plots, alpha diversity measurements plots, the bar plot for the classification of the microbial community at phylum level for different soils and treatments and for exporting a subset of OTUs information based on the variables in metadata. Vegan was used to test differences between microbial

communities with Permutational Multivariate Analysis of Variance (PERMANOVA). Ampvis2 was used to generate the rarefaction curves and heatmaps of average abundance at the genus level of the sample replicates. OTUs with at least 0.06% average relative abundance and 50% occurrence were selected for building the correlation network. The packages Hmisc and Matrix were used to calculate the correlation of OTUs with Spearman correlation. Strong correlations (correlation coefficient ≥ 0.7) and Benjamini-Hochberg method adjusted p value ($p < 0.01$) were set to filter the correlation result. The filtered correlation result were used to build occurrence network with the package igraph and these were visualized in Gephi (Bastian et al., 2006).

The OTUs enriched in the heavy fractions of the ^{13}C labeled cDCE or 1,4-dioxane amended microcosms were determined using STAMP. Specifically, OTU relative abundance was compared between the heavy fractions of the microcosms amended with the labeled chemical and the heavy fractions of the microcosms amended with the unlabeled chemical (Welch's two-sided t-test, $p < 0.05$, with default settings). STAMP was also used to investigate which OTUs were enriched in the light fractions of the labeled amended microcosms compared to the light fractions of the unlabeled amended microcosms to eliminate false positives in the heavy fraction analysis. In addition, the enriched OTUs were subject to further statistical analysis in RStudio (Wilcoxon Rank Test, ggplot2 and ggpubr).

2.6 Function prediction and correlation

The microbial functions from KEGG orthologs (KO) (Kanehisa et al., 2016) were predicted from the sequencing data using the PICRUSt2 pipeline (Douglas et al., 2020). PICRUSt2 applied with EPA-NG (Barbera et al., 2019) and gappa (Czech et al., 2020) for phylogenetic placement of reads, castor (Louca and Doebeli, 2018) for hidden state prediction and MinPath (Ye and Doak, 2009) for pathway inference. The functions related to 1,4-dioxane and cDCE degradation identified in previous research were manually picked (Giddings et al., 2010; Grostern et al., 2012; He et al., 2017; Mahendra and Alvarez-Cohen, 2006; Nishino et al., 2013; Semprini, 1997; Van Hylckama et al., 1997) to generate the heatmaps of relative abundance across all sample replicates with the R package ComplexHeatmap (Gu et al., 2016) (version 2.4.3). In addition, OTUs from 1,4-dioxane and cDCE SIP experiments with an average relative abundance $\geq 0.05\%$ were collected and pooled together with functions associated with 1,4-dioxane and cDCE

degradation for running Spearman correlations. OTUs correlated with at least 4 and 2 functions for 1,4-dioxane and cDCE degradation, respectively, with absolute values of correlation coefficients higher than 0.6 were chosen for plotting the heatmaps with the same R package.

2.7 Species associated with 1,4-dioxane and DCE degradation

Previously, our group submitted DNA extracts from the same soils (Treatments 1 and 2 from KBS) for shotgun sequencing (Thelusmond et al., 2019). In the current work, the shotgun sequences (processed by Trimmomatic (Bolger et al., 2014)) were assembled with Megahit (Li et al., 2016) (version 1.2.4) using the pair end plus single end option. Minimum and maximum kmer sizes were 27 and 127 with the kmer size step of 10. Previously identified 1,4-dioxane and cDCE degraders were searched for in the National Center for Biotechnology Information (NCBI) taxonomy browser to find their lowest ranks (primarily rank of species) and taxonomy IDs (Supplementary Table 1). The assembled reads were then aligned to the NCBI nucleotide database (nt) with the taxids option in BLASTN (Altschul et al., 1990) (version 2.10.0-Linux_x86_64). The results were restricted to evalue $\leq 1\times 10^{-5}$ (with output format 6) and identity ≥ 60 % and the resulting files were then imported into Megan (Huson et al., 2016) (community edition version 6.19.7). Each BLASTN output was processed to map the Megan genomic DNA accession database for generating the phylogenetic trees of the species associated with 1,4-dioxane or DCE degradation.

3. Results

3.1 Degradation of 1,4-Dioxane and cDCE with or without lactate

1,4-Dioxane and cDCE concentrations were determined in microcosms with inocula from two soils, with or without the additional amendment(s) of lactate/1,4-dioxane/cDCE (Figures 1 and 2). For soil 1 inoculated microcosms, when all three substrates were added together, the differentiation between removal trends for 1,4-dioxane between the samples and abiotic controls was not strong, with 95% confidence intervals (CIs) for the regression lines overlapping the entire course of the incubation (Figure 1A, part A). However, when only lactate was added, the 1,4-dioxane regression lines 95% CIs between the abiotic controls and samples separated before day 20 (Figure 1A, part B). Similarly, when only cDCE was added, the 1,4-dioxane regression lines 95% CIs between the samples and abiotic controls separated at ~ day 20 (Figure 1, part C).

Based on these trends, for this particular microbial community, one hypothesis is that when all three substrates are present, 1,4-dioxane removal is slower (Figure 1A, part A). Compared to soil 1 microcosms, the impact of additional chemicals on 1,4-dioxane removal was different for soil 2 microcosms. That is, 1,4-dioxane biodegradation was similar for all three treatments, indicating the present of either lactate or cDCE or both did not impact 1,4-dioxane removal in this soil community (Figure 2A, parts A-C).

The most notable trend for cDCE biodegradation in both soil 1 and soil 2 microcosms concerns the addition of lactate. In soil 1 microcosms, there was no overlap between the regression line 95% CIs of the samples and controls when lactate was present (Figure 1B, part A), however when lactate was absent, the 95% CIs did not separate until ~day 20 (Figure 1B, part C), suggesting a delayed on-set of cDCE degradation. In soil 2 microcosms, the overlap between the 95% CIs remained until ~ day 40 when lactate was absent (Figure 2B, part C, compared to ~ day 10 for both of the lactate amended treatments (Figure 2B, parts A and B). The trends for both soils support the hypothesis that the presence of lactate accelerates the initiation of cDCE biodegradation. Based on these results, lactate was added to the cDCE SIP experiments but not to the 1,4-dioxane SIP experiments.

For soil 1 microcosms, the cDCE regression line slopes were similar (0.022 vs. 0.021) when either lactate was added with 1,4-dioxane (Figure 1B, part A), or when only lactate was added (Figure 1B, part B), suggesting 1,4-dioxane does not impact cDCE removal in this soil community. For soil 2 microcosms, the cDCE regression line slopes were also similar (0.022 vs. 0.017) when either lactate was added with 1,4-dioxane (Figure 2B, part A), or when lactate was added by itself (Figure 2B, part B), again suggesting 1,4-dioxane likely does not impact cDCE removal (when lactate is present). In microcosms amended with all three substrates, decreases in cDCE concentrations occurred earlier than decreases for 1,4-dioxane in both soils 1 and 2 (as shown by an earlier separation of the regression line 95% CIs between the samples and controls, Figure 1A, B, part A, Figure 2A, B part A). The pattern suggests there is a sequential removal for cDCE and 1,4-dioxane with the addition of lactate. In comparison, when the microcosms were amended with only 1,4-dioxane and cDCE (Figure 1A, B, part C, Figure 2A, B part C) the trend

was less clear. In soil 2 microcosms, 1,4-dioxane removal started before cDCE removal while in soil 1 microcosms, the removal for 1,4-dioxane and cDCE started at a similar time.

The SIP experiments involved the addition of cDCE and 1,4-dioxane separately to microcosms inoculated with each soil (Supplementary Figure 1). Triplicate samples for each were sacrificed at 44 days for DNA extraction (~50% removal of 1,4-dioxane or cDCE). The concentration of cDCE in abiotic controls declined towards the end of the study, likely a result of gas phase leakage through the previously punctured rubber septa (the septa were punctured multiple times to remove samples for GC analysis). (Supplementary Figure 1 C and D).

3.2 Microbial community analysis

The rarefaction curves of the SIP fractions plateaued, indicating the majority of the species were sequenced (Supplementary Figure 2). A larger number of species were found in microcosms amended with soil 2 from all fractions (Supplementary Figure 2). The NMDS analysis suggested the community composition was different between the light and heavy fractions in both the cDCE (Figure 3A) and 1,4-dioxane (Figure 3B) amended microcosms, indicating a successful fractionation process. While a clear separation between the two soils was visible in the fractions originating from the cDCE amendments (Figure 3A), the separation was less pronounced in the 1,4-dioxane fractions (Figure 3B), suggesting a greater similarity in the latter samples. The differences of the microbial communities from heavy and light fractions were validated by PERMANOVA (p-value of 0.01, Supplementary Table 2). Alpha diversity and richness indices (Figure 3C and D) indicated a greater distinction between the light and heavy fractions of the cDCE amended samples compared to those amended with 1,4-dioxane. NMDS analysis also provided clear distinctions between the communities based on the amended substrate (cDCE or 1,4-dioxane) (Supplementary Figure 3). The diversity and richness indices were higher in the samples amended with cDCE compared to those amended with 1,4-dioxane (Supplementary Figure 3).

Using the rarefied even depth of 95% of the minimum sum of OTU counts, 32 phyla were identified (Figure 4A). Major phyla included *Proteobacteria* and *Actinobacteria*, and these were more abundant in all heavy fractions compared to the light fractions, while *Bacteroidetes* was

dominant in the light fractions. *Gemmatimonadetes* was more abundant in the heavy fractions only in the cDCE amended samples. Other major phyla included *Chloroflexi, Firmicutes* and *Verrucomicrobia*. In many cases, a clear distinction is visible between the ^{12}C and ^{13}C amended fractions, indicating differences between communities, as discussed below.

As *Proteobacteria* represented the phylum with the greatest number of sequences, the most abundant families (top 30 OTUs) within this phylum were determined (Figure 4B). Those that illustrated a higher abundance in the cDCE amended samples included*: Bacteriovoracaceae, Bdellovibrionaceae, CCD24_fa, Chromobacteriaceae, Deltaproteobacteria_*unclassified*, Pseudomonadaceae, Sphingomonadaceae* and *Steroidobacteraceae*. In the 1,4-dioxane amended samples, *Rhodanobacteraceae* was more abundant and several samples illustrated a high abundance of *Burkholderiaceae* and *Xanthobacteraceae*. At the genus level for all phyla, the most abundant genera in the 1,4-dioxane amended samples classified as *Rhodanobacter*, *Chujaibacter* (both *Proteobacteria*) and an uncharacterized genus within *Bacteroidetes* (Supplementary Figure 4). While in the cDCE amended samples, the most abundant genera included unclassified *Bacteria*, *Pseudomonas* (*Proteobacteria*) and *Gp6* (*Actinobacteria*) (Supplementary Figure 4). The current work also involved the analysis of shotgun sequencing data from the same two soils from a previous study (Thelusmond et al., 2019). Here, multiple species previously associated with 1,4-dioxane and cDCE degradation were identified, including *Pseudonocardia dioxanivorans* (1,4-dioxane degrader) and *Polaromonas* sp. JS666 (cDCE degrader) (Supplementary Figure 5).

3.3 Phylotypes responsible for ^{13}C uptake from cDCE and 1,4-Dioxane

Phylotypes enriched in the heavy fractions of the ^{13}C cDCE or ^{13}C 1,4-dioxane amended samples compared to the controls (heavy fractions from ^{12}C cDCE or ^{12}C 1,4-dioxane amended samples) were determined using Welch's two sided t-test (within STAMP, $p < 0.05$) (Supplementary Figure 6 and 7). The dominant enriched genera for ^{13}C uptake from 1,4-dioxane included *Rhodopseudomonas* and *Rhodanobacter* (Supplementary Figure 6). Whereas the dominant enriched genera for ^{13}C uptake from cDCE included *Bacteriovorax*, *Pseudomonas* and *Sphingomonas* (Supplementary Figure 7). An additional statistical test (Wilcoxon Rank, $p < 0.05$) confirmed the enrichment of *Rhodopseudomonas* and *Rhodanobacter* in one or both

replicates of both soils (Figure 5). For cDCE, multiple genera were enriched in replicates of soil 1 and 2 (Figure 6). Enriched genera in soil 1 included: *Bacteriovorax*, *Bradyrhizobium* and two unclassified genera from *Blastocatellaceae*. Enriched genera in soil 2 included: *Bradyrhizobium*, *Caulobacter*, an uncultured genus within *Vicinamibacterales*, *Pseudomonas* and *Sphingomonas*. The greater diversity of dominant enriched OTUs in cDCE microcosms between soils, compared to 1,4-dioxane microcosms between soils, is consistent with the NMDS analysis indicating clear distinctions between cDCE communities between soils compared to 1,4-dioxane communities between soils (Figure 3).

3.4 Co-occurrence networks

Co-occurrence networks were generated to illustrate the differences between soil 1 and soil 2 microbial communities involved in 1,4-dioxane and cDCE degradation (those enriched in ^{13}C heavy fractions, STAMP analysis) (Supplementary Figure 8). The OTUs with a correlation coefficient > 0.7 were connected with lines. The main genera were represented by 166 and 172 nodes (analyzed as OTUs present in at least 50% of the samples and with the abundance ≥ 0.06%) for the degradation of 1,4-dioxane and cDCE, respectively. For the microbial communities associated with 1,4-dioxane biodegradation, 67 OTUs showed a significant difference between soil 1 and 2 (26 and 41 were more abundant in soil 1 and soil 2, respectively) (Supplementary Figure 8 A). In contrast, more OTUs (99) illustrated a significant difference between the soil 1 and soil 2 microbial communities for those involved in cDCE biodegradation (44 and 45 OTUs were more abundant in soil 1 and 2, and these OTUs were clearly separated) (Supplementary Figure 8 B).

The network also illustrated the relationships between the enriched and other abundant OTUs. The enriched OTUs (by STAMP analysis) displayed on the networks are summarized (Supplementary Table 3). In the microbial communities associated with 1,4-dioxane biodegradation, the majority of OTUs classified as *Actinobacteria*, *Proteobacteria* and *Acidobacteria* (Supplementary Figure 9A). *Actinobacteria* and *Proteobacteria* were related to each other. A total of 58 and 8 enriched OTUs were displayed in soil 1 and 2, respectively. Most of the enriched OTUs were *Actinobacteria* and *Proteobacteria* (Supplementary Figure 9B). In the microbial communities associated with cDCE biodegradation, the majority of the OTUs were

Proteobacteria, *Bacteroidetes*, *Acidobacteria* and *Gemmatimonadetes* (Supplementary Figure 10A). *Proteobacteria* connected more with *Gemmatimonadetes.* A total of 26 and 16 enriched OTUs were displayed in soil 1 and 2, respectively. The enriched OTUs were *Bacteroidetes*, *Acidobacteria* in soil 1 while the enriched OTUs were *Proteobacteria* in soil 2 (Supplementary Figure 10B).

3.5 Predicted functions and correlations with OTUs

In the current work, PICRUSt2 predicted KO functions formerly associated with 1,4-dioxane biodegradation in the 1,4-dioxane amended microcosms included toluene monooxygenase, propane monooxygenase (most abundant) and methane monooxygenase (He et al., 2017; Mahendra and Alvarez-Cohen, 2006) (Supplementary Figure 11). In the cDCE amended microcosms, the abundant function associated with cDCE included glutathione S-transferase (Giddings et al., 2010; Jennings et al., 2009). For 1,4-dioxane, correlations between gene and phylotype abundance indicated propane monooxygenase positively correlated with *Rokubacteriales*, *KD4-96* (*Chloroflexi*), Gitt-GS-36 (*Chloroflexi*) and uncultured genera from *Vicinamibacterales* and *Gemmatimonadaceae* (Figure 7A). For cDCE, glutathione S-transferase was positively correlated with *BIrii4* and an unclassified genus from *Xanthomonadales* (Figure 7B).

4. Discussion

There have been many reports of the common occurrence of TCE and 1,4-dioxane at contaminated sites (Adamson et al., 2014; Anderson et al., 2012; Li et al., 2021). As TCE is reduced to cDCE by both indigenous microbial communities or dechlorinating cultures (Ellis et al., 2000; Fennell et al., 2001; Li et al., 2021; Polasko et al., 2019) and "cDCE-stall" is common at contaminated sites the removal of this metabolite is also of concern. Previously, we reported 1,4-dioxane biodegradation in the two soils examined here (Ramalingam and Cupples, 2020). Here, we build on that research by investigating the potential for the concurrent biodegradation of both cDCE and 1,4-dioxane. Further, the microorganisms involved in the uptake of carbon from each chemical were identified using DNA-based SIP. Additionally, the functional genes involved in the degradation of cDCE and 1,4-dioxane were predicted using PICRUSt2 (Douglas et al., 2020) and their abundance was correlated to OTUs present.

The impact of additional treatments on 1,4-dioxane biodegradation differed between the two soils. For soil 1, when all three substrates were present (lactate, cDCE and 1,4-dioxane), 1,4-dioxane removal was slower. However, in soil 2, 1,4-dioxane biodegradation was similar for all three treatments, indicating the present of either lactate or cDCE or both did not impact 1,4-dioxane removal in this soil community. Inhibition of 1,4-dioxane biodegradation by additional substrates has been noted by others. For example, when propane was added to *Azoarcus* sp. DD4, co-metabolism of 1,4-dioxane was delayed and followed the co-metabolism of chloroethenes (1,1-dichlorothene, VC and cDCE) (Deng et al., 2018; Li et al., 2021). Further, research with *Pseudonocardia dioxanivorans* CB1190 indicated from four common co-contaminants (1,1-DCE, 1,1,1-TCA, cDCE, TCE), cDCE was the second most inhibitory chemical to aerobic 1,4-dioxane degradation (Zhang et al., 2016).

The most notable trend for cDCE removal was the positive impact of lactate. Also, when lactate was present, 1,4-dioxane did not impact cDCE removal and decreases in cDCE concentrations occurred earlier than 1,4-dioxane decreases in both soil microcosms. In comparison, when the microcosms were amended with only 1,4-dioxane and cDCE the trend was less clear. In soil 2 microcosms, 1,4-dioxane removal started before cDCE removal while in soil 1 microcosms, the removal for 1,4-dioxane and cDCE started at a similar time.

Unlike previous studies which have primarily involved the biodegradation of co-contaminants by isolates or commercially available mixed communities (Deng et al., 2018; Li et al., 2021; Polasko et al., 2019), this work examined contaminant biodegradation by indigenous microbial communities. The NMDS analysis indicated cDCE produced a clear difference between the microbial communities of the two soils. The difference between the two microbial communities was less distinct for the soil microcosms amended with 1,4-dioxane. These trends could suggest cDCE is more important for impacting microbial community structure, perhaps through inhibition or as a beneficial substrate. Interestingly, the microbial richness and diversity levels were also higher in the cDCE amended samples. Also, the enriched phylotypes illustrated greater differences between soils in the cDCE amended microcosms, compared to the 1,4-dioxane amended microcosms.

To date, many aerobic 1,4-dioxane and cDCE degraders have been identified (Supplementary Table 1). In the current study, multiple 1,4-dioxane and cDCE degraders were detected in shotgun sequencing data from samples inoculated with both soils. To determine if these species were actively involved in biodegradation, SIP was employed to determine which microorganisms were responsible for carbon uptake from each chemical. From the twelve 1,4-dioxane degrading phylotypes identified by shotgun sequencing, only two were associated with carbon uptake from 1,4-dioxane. Specifically, the previously reported 1,4-dioxane degraders *Rhodanobacter* sp. and *Xanthobacter flavus* were detected via shotgun sequencing and OTUs classifying as *Rhodanobacter* and the family *Xanthobacteraceae* were detected via SIP. From the nineteen cDCE degrading phylotypes detected via shotgun sequencing only one genus (*Pseudomonas*) was detected via SIP. These results provide support for the importance of SIP, over sequencing alone, for connecting identity with function.

In the current work, many genera were enriched during the SIP experiments, suggesting a wide range of microorganisms were assimilating carbon from the biodegradation of 1,4-dioxane or cDCE. Significantly enriched genera from the biodegradation of ^{13}C-1,4-dioxane included *Rhodopseudomonas* and *Rhodanobacter*. Consistent with the current study, *Rhodopseudomonas* was previously associated with the incorporation of ^{13}C from 1,4-dioxane in aerobic experiments with activated sludge, and its abundance increased with the degradation of 1,4-dioxane in both batch tests and a full-scale treatment system (Aoyagi et al., 2018). *Rhodanobacter* was also reported as a metabolizer for 1,4-dioxane, with the addition of tetrahydrofuran accelerating 1,4-dioxane degradation (Pugazhendi, 2015). Combined with the results from the current work, these studies indicate the importance of both genera for 1,4-dioxane biodegradation and future work should examine their occurrence and activity at 1,4-dioxane contaminated sites.

The other SIP identified genera during 1,4-dioxane degradation illustrated lower relative abundance levels compared to *Rhodopseudomonas* and *Rhodanobacter.* An OTU classifying as *Afipia* was enriched in microcosms inoculated with soil 2. Similarly, others have linked this genus (*Afipia* sp. D1) to the assimilation of carbon from 1,4-dioxane (Sei et al., 2013). *Afipia* was also abundant in uncontaminated soil microcosms during 1,4-dioxane degradation (He et al., 2018; Nam et al., 2016). Here, an unclassified genus from *Xanthobacteraceae* was associated

with carbon uptake from 1,4-dioxane in soil 1 microcosms. This family includes the 1,4-dioxane degraders *Xanthobacter* sp. YN2 (Ma et al., 2021) and *Xanthobacter flavus* DT8 (Chen et al., 2016). *Xanthobacteraceae* significantly increased in 1,4-dioxane degradation tests with domestic wastewater activated sludge, and a novel 1,4-dioxane-hydroxylating monooxygenase was identified from *Xanthobacter* strains (Chen et al., 2021). Another enriched OTU from the 1,4-dioxane SIP study classified within the family *Xanthomonadaceae*. This family was previously linked to 1,4-dioxane degradation in activated sludge from a full-scale bioreactor for landfill leachate treatment (Xiong et al., 2020; Xiong et al., 2019). In other 1,4-dioxane degradation studies, dominant or enriched genera included *Chryseobacterium*, *Dokdonella*, *Pseudonocardia*, *Bradyrhizobium*, *Mycobacterium*, *Nocardioides*, and *Kribbella* (Ramalingam and Cupples, 2020; Tusher et al., 2019), however these genera were not identified via SIP in the current work.

Dominant genera significantly enriched in the biodegradation of ^{13}C-cDCE in either or both soil microcosms and replicates, included *Bacteriovorax*, *Pseudomonas* and *Sphingomonas*. The dominance of *Pseudomonas* is consistent with previous studies associating this genus with cDCE degradation (Supplementary Table 1). Although isolates from the genus *Bacteriovorax* have not been previously linked with cDCE biodegradation, this genus has previously been associated with hydrocarbon biodegradation (Bacosa et al., 2018; Hu et al., 2017). In the current work, two enriched genera (*Sphingomonas* and *Bradyrhizobium*) during ^{13}C-cDCE degradation were abundant or enriched in previous 1,4-dioxane degradation studies (Miao et al., 2019; Miao et al., 2020; Xiong et al., 2020). *Sphingomonas* was dominant during 1,4-dioxane by *P. dioxanivorans* CB1190 when residuals of chlorinated volatile organic compounds (including cDCE) were present (Miao et al., 2019; Miao et al., 2020). However, in the current study, these genera were not associated with ^{13}C uptake from 1,4-dioxane. Interestingly, there were multiple novel genera, with no previous links to cDCE or 1,4-dioxane, identified in the current study as carbon assimilators.

Multiple functions for 1,4-dioxane and cDCE biodegradation were predicted in the soil microcosms using PICRUSt2 (Douglas et al., 2020). The most abundant function for 1,4-dioxane biodegradation was propane monooxygenase. Many OTUs positively correlated with propane monooxygenase, including for example *KD4-96* (*Chloroflexi*), an uncultured genus from the

class of *Vicinamibacterales* and from the family of *Gemmatimonadaceae*. The high abundance of propane monooxygenase is consistent with previous work describing the dominance of propane monooxygenase from *Rhodococcus jostii* RHA1 and *Rhodococcus* sp. RR1 in 1,4-dioxane degrading microcosms inoculated with these soils (Ramalingam and Cupples, 2020). Several other previously identified 1,4-dioxane degrading enzymes were predicted to be present in the soil microcosms, however, additional research is needed to confirm if these enzymes are active. The functional genes associated with aerobic cDCE degradation include cytochrome P450 monooxygenase and glutathione S-transferase *Polaromonas* sp. strain JS666 (Giddings et al., 2010; Jennings et al., 2009; Nishino et al., 2013). In the current study, both biomarkers correlated with a number of OTUs, but not *Polaromonas* strain JS666. However, these OTUs were not enriched in the SIP experiments, suggesting other enzymes may be involved or other methods (beyond the predictions provided by PICRUSt) are needed to obtain such information. Combining the current research with more quantitative approaches (e.g. qPCR, RNA-Seq) would enhance the information gained from the functional gene analysis.

5. Conclusions

This work demonstrated the concurrent removal of cDCE and 1,4-dioxane by indigenous soil microbial communities and the enhancement of the on-set of cDCE removal by the addition of lactate. Through the use of SIP, multiple genera, both previously identified and not previously identified degraders, were enriched and benefited from the degradation of 1,4-dioxane and cDCE. In addition, a wide range of genes involved in the degradation were predicted to be associated with contaminant removal. These genera and genes were more diverse than previously reported. The extraction of DNA at only one time point during biodegradation is a potential limitation of the current study. Further, it is unknown if the enriched genera participated in carbon uptake from 1,4-dioxane and cDCE, or from their metabolites. The data generated in the current study has the potential to be incorporated into diagnostic tests for assessing biodegradation potential at contaminated sites, for example, quantification of *Rhodopseudomonas* and *Rhodanobacter* at 1,4-dioxane contaminated sites. This is a key study to illustrate the potential of naturally occurring mixed communities to degrade both contaminants. To date, research directed towards the co-contamination problem concerns isolates or commercial cultures. If both chemicals can degrade concurrently without any bioaugmentation,

this has significant consequences for the remediation industry. Although the results suggest concurrent biodegradation of cDCE and 1,4-dioxane should be considered for chlorinated solvent site remediation, additional research is needed to determine if appropriately low contaminant concentrations can be reached.

Acknowledgements

Thanks to Stacey VanderWulp from MSU for providing the soil samples from KBS LTER. This work was partially supported by NSF grant number 1902250.

Reference

Adamson DT, Mahendra S, Walker KL, Rauch SR, Sengupta S, Newell CJ. A Multisite Survey To Identify the Scale of the 1,4-Dioxane Problem at Contaminated Groundwater Sites. Environmental Science & Technology Letters 2014; 1: 254-258.

Altschul SF, Gish W, Miller W, Myers EW, Lipman DJ. Basic local alignment search tool. J Mol Biol 1990; 215: 403-10.

Andersen KS, Kirkegaard RH, Karst SM, Albertsen M. ampvis2: an R package to analyse and visualise 16S rRNA amplicon data. bioRxiv 2018: 299537.

Anderson RH, Anderson JK, Bower PA. Co-occurrence of 1,4-dioxane with trichloroethylene in chlorinated solvent groundwater plumes at US Air Force installations: Fact or fiction. Integrated Environmental Assessment and Management 2012; 8: 731-737.

Aoyagi T, Morishita F, Sugiyama Y, Ichikawa D, Mayumi D, Kikuchi Y, et al. Identification of active and taxonomically diverse 1,4-dioxane degraders in a full-scale activated sludge system by high-sensitivity stable isotope probing. ISME J 2018; 12: 2376-2388.

Bacosa HP, Erdner DL, Rosenheim BE, Shetty P, Seitz KW, Baker BJ, et al. Hydrocarbon degradation and response of seafloor sediment bacterial community in the northern Gulf of Mexico to light Louisiana sweet crude oil. ISME J 2018; 12: 2532-2543.

Barbera P, Kozlov AM, Czech L, Morel B, Darriba D, Flouri T, et al. EPA-ng: Massively Parallel Evolutionary Placement of Genetic Sequences. Syst Biol 2019; 68: 365-369.

Bastian M, Heymann S, Jacomy M. Gephi: an open source software for exploring and manipulating networks. International AAAI Conference on Weblogs and Social Media 2006.

Bates D, Maechler M, Davis TA, Oehlschlägel J, Riedy J. Matrix: sparse and dense matrix classes and methods, 2019.

Bolger AM, Lohse M, Usadel B. Trimmomatic: a flexible trimmer for Illumina sequence data. Bioinformatics 2014; 30: 2114-20.

Brown RA, Mueller JG, Seech AG, Henderson JK, Wilson JT. Interactions between biological and abiotic pathways in the reduction of chlorinated solvents. Remediation Journal 2009; 20: 9-20.

Chen D-Z, Jin X-J, Chen J, Ye J-X, Jiang N-X, Chen J-M. Intermediates and substrate interaction of 1,4-dioxane degradation by the effective metabolizer *Xanthobacter flavus* DT8. International Biodeterioration & Biodegradation 2016; 106: 133-140.

Chen R, Miao Y, Liu Y, Zhang L, Zhong M, Adams JM, et al. Identification of novel 1,4-dioxane degraders and related genes from activated sludge by taxonomic and functional gene sequence analysis. J Hazard Mater 2021; 412: 125157.

Cho K-C, Lee DG, Roh H, Fuller ME, Hatzinger PB, Chu K-H. Application of 13C-stable isotope probing to identify RDX-degrading microorganisms in groundwater. Environmental Pollution 2013; 178: 350-360.

Csardi G, Nepusz T. The igraph software package for complex network research. InterJournal, Complex Systems 2006; 1695.

Czech L, Barbera P, Stamatakis A. Genesis and Gappa: processing, analyzing and visualizing phylogenetic (placement) data. Bioinformatics 2020; 36: 3263-3265.

Deng D, Li F, Wu C, Li M. Synchronic Biotransformation of 1,4-Dioxane and 1,1-Dichloroethylene by a Gram-Negative Propanotroph *Azoarcus* sp. DD4. Environmental Science & Technology Letters 2018; 5: 526-532.

Douglas GM, Maffei VJ, Zaneveld JR, Yurgel SN, Brown JR, Taylor CM, et al. PICRUSt2 for prediction of metagenome functions. Nat Biotechnol 2020; 38: 685-688.

Ellis DE, Lutz EJ, Odom JM, Buchanan RJ, Bartlett CL, Lee MD, et al. Bioaugmentation for Accelerated In Situ Anaerobic Bioremediation. Environmental Science & Technology 2000; 34: 2254-2260.

EPA. Technical Fact Sheet - 1,4-Dioxane, 2017.

Fennell DE, Carroll AB, Gossett JM, Zinder SH. Assessment of Indigenous Reductive Dechlorinating Potential at a TCE-Contaminated Site Using Microcosms, Polymerase Chain Reaction Analysis, and Site Data. Environmental Science & Technology 2001; 35: 1830-1839.

Freedman DL, Gossett JM. Biological reductive dechlorination of tetrachloroethylene and trichloroethylene to ethylene under methanogenic conditions. Appl Environ Microbiol 1989; 55: 2144-51.

Giddings CGS, Jennings LK, Gossett JM. Microcosm Assessment of a DNA Probe Applied to Aerobic Degradation of cis-1,2-Dichloroethene by *Polaromonas* sp. Strain JS666. Groundwater Monitoring & Remediation 2010; 30: 97-105.

Gossett JM. Measurement of Henry's law constants for C1 and C2 chlorinated hydrocarbons. Environmental Science & Technology 1987; 21: 202-208.

Grostern A, Sales CM, Zhuang W-Q, Erbilgin O, Alvarez-Cohen L. Glyoxylate Metabolism Is a Key Feature of the Metabolic Degradation of 1,4-Dioxane by Pseudonocardia dioxanivorans Strain CB1190. Applied and Environmental Microbiology 2012; 78: 3298.

Gu Z, Eils R, Schlesner M. Complex heatmaps reveal patterns and correlations in multidimensional genomic data. Bioinformatics 2016; 32: 2847-9.

Harrell FE. Hmisc: harrell miscellaneous, 2020.

He Y, Mathieu J, da Silva MLB, Li M, Alvarez PJJ. 1,4-Dioxane-degrading consortia can be enriched from uncontaminated soils: prevalence of *Mycobacterium* and soluble di-iron monooxygenase genes. Microbial Biotechnology 2018; 11: 189-198.

He Y, Mathieu J, Yang Y, Yu P, da Silva MLB, Alvarez PJJ. 1,4-Dioxane Biodegradation by *Mycobacterium dioxanotrophicus* PH-06 Is Associated with a Group-6 Soluble Di-Iron Monooxygenase. Environmental Science & Technology Letters 2017; 4: 494-499.

Hu P, Dubinsky EA, Probst AJ, Wang J, Sieber CMK, Tom LM, et al. Simulation of Deepwater Horizon oil plume reveals substrate specialization within a complex community of hydrocarbon degraders. Proceedings of the National Academy of Sciences 2017; 114: 7432-7437.

Huson DH, Beier S, Flade I, Gorska A, El-Hadidi M, Mitra S, et al. MEGAN community edition - interactive exploration and analysis of large-Scale microbiome sequencing data. PLoS Comput Biol 2016; 12: e1004957.

Jayamani I, Cupples AM. Stable isotope probing reveals the importance of *Comamonas* and *Pseudomonadaceae* in RDX degradation in samples from a Navy detonation site. Environ Sci Pollut Res Int 2015; 22: 10340-50.

Jennings LK, Chartrand MM, Lacrampe-Couloume G, Lollar BS, Spain JC, Gossett JM. Proteomic and transcriptomic analyses reveal genes upregulated by cis-dichloroethene in *Polaromonas* sp. strain JS666. Appl Environ Microbiol 2009; 75: 3733-44.

Kanehisa M, Sato Y, Kawashima M, Furumichi M, Tanabe M. KEGG as a reference resource for gene and protein annotation. Nucleic Acids Res 2016; 44: D457-62.

Kassambara A. ggpubr: 'ggplot2' Based Publication Ready Plots., 2020.

Kozich JJ, Westcott SL, Baxter NT, Highlander SK, Schloss PD. Development of a dual-index sequencing strategy and curation pipeline for analyzing amplicon sequence data on the MiSeq Illumina sequencing platform. Appl Environ Microbiol 2013; 79: 5112-20.

Lahti L, Shetty S. Tools for microbiome analysis in R, 2017.

Li D, Luo R, Liu CM, Leung CM, Ting HF, Sadakane K, et al. MEGAHIT v1.0: A fast and scalable metagenome assembler driven by advanced methodologies and community practices. Methods 2016; 102: 3-11.

Li F, Deng D, Zeng L, Abrams S, Li M. Sequential anaerobic and aerobic bioaugmentation for commingled groundwater contamination of trichloroethene and 1,4-dioxane. Sci Total Environ 2021; 774: 145118.

Louca S, Doebeli M. Efficient comparative phylogenetics on large trees. Bioinformatics 2018; 34: 1053-1055.

Ma F, Wang Y, Yang J, Guo H, Su D, Yu L. Degradation of 1,4-Dioxane by *Xanthobacter* sp. YN2. Curr Microbiol 2021; 78: 992-1005.

Mahendra S, Alvarez-Cohen L. Kinetics of 1,4-dioxane biodegradation by monooxygenase-expressing bacteria. Environ Sci Technol 2006; 40: 5435-42.

Mahendra S, Grostern A, Alvarez-Cohen L. The impact of chlorinated solvent co-contaminants on the biodegradation kinetics of 1,4-dioxane. Chemosphere 2013; 91: 88-92.

McMurdie PJ, Holmes S. phyloseq: an R package for reproducible interactive analysis and graphics of microbiome census data. PLoS One 2013; 8: e61217.

Miao Y, Johnson NW, Gedalanga PB, Adamson D, Newell C, Mahendra S. Response and recovery of microbial communities subjected to oxidative and biological treatments of 1,4-dioxane and co-contaminants. Water Research 2019; 149: 74-85.

Miao Y, Johnson NW, Phan T, Heck K, Gedalanga PB, Zheng X, et al. Monitoring, assessment, and prediction of microbial shifts in coupled catalysis and biodegradation of 1,4-dioxane and co-contaminants. Water Research 2020; 173: 115540.

Myers MA, Johnson NW, Marin EZ, Pornwongthong P, Liu Y, Gedalanga PB, et al. Abiotic and bioaugmented granular activated carbon for the treatment of 1,4-dioxane-contaminated water. Environ Pollut 2018; 240: 916-924.

Nam JH, Ventura JS, Yeom IT, Lee Y, Jahng D. Structural and Kinetic Characteristics of 1,4-Dioxane-Degrading Bacterial Consortia Containing the Phylum TM7. J Microbiol Biotechnol 2016; 26: 1951-1964.

Nishino SF, Shin KA, Gossett JM, Spain JC. Cytochrome P450 initiates degradation of cis-dichloroethene by Polaromonas sp. strain JS666. Appl Environ Microbiol 2013; 79: 2263-72.

Oksanen J, Blanchet FG, Friendly M, Kindt R, Legendre P, McGlinn D, et al. vegan: Community Ecology Package, 2020.

Paes F, Liu X, Mattes TE, Cupples AM. Elucidating carbon uptake from vinyl chloride using stable isotope probing and Illumina sequencing. Applied Microbiology and Biotechnology 2015; 99: 7735-7743.

Parales RE, Adamus JE, White N, May HD. Degradation of 1,4-dioxane by an Actinomycete in pure culture. Appl Environ Microbiol 1994; 60: 4527-30.

Parks DH, Tyson GW, Hugenholtz P, Beiko RG. STAMP: statistical analysis of taxonomic and functional profiles. Bioinformatics 2014; 30: 3123-4.

Polasko AL, Zulli A, Gedalanga PB, Pornwongthong P, Mahendra S. A Mixed Microbial Community for the Biodegradation of Chlorinated Ethenes and 1,4-Dioxane. Environmental Science & Technology Letters 2019; 6: 49-54.

Pruesse E, Quast C, Knittel K, Fuchs BM, Ludwig W, Peplies J, et al. SILVA: a comprehensive online resource for quality checked and aligned ribosomal RNA sequence data compatible with ARB. Nucleic Acids Res 2007; 35: 7188-96.

Pugazhendi A. Biodegradation of 1,4-dioxane by *Rhodanobacter* AYS5 and the role of additional substrates. Annals of Microbiology 2015; 65.

R Core Team. R: A language and environment for statistical computing. R Foundation for Statistical Computing, Vienna, Austria. , 2018.

Radajewski S, Ineson P, Parekh NR, Murrell JC. Stable-isotope probing as a tool in microbial ecology. Nature 2000; 403: 646-649.

Ramalingam V, Cupples AM. Enrichment of novel Actinomycetales and the detection of monooxygenases during aerobic 1,4-dioxane biodegradation with uncontaminated and contaminated inocula. Appl Microbiol Biotechnol 2020; 104: 2255-2269.

RStudio Team. RStudio: Integrated Development for R. RStudio, PBC. Boston, MA, 2020.

Schloss PD. A high-throughput DNA sequence aligner for microbial ecology studies. PLoS One 2009; 4: e8230.

Sei K, Miyagaki K, Kakinoki T, Fukugasako K, Inoue D, Ike M. Isolation and characterization of bacterial strains that have high ability to degrade 1,4-dioxane as a sole carbon and energy source. Biodegradation 2013; 24: 665-674.

Semprini L. Strategies for the aerobic co-metabolism of chlorinated solvents. Curr Opin Biotechnol 1997; 8: 296-308.

Steffan RJ, Vainberg S. Production and handling of *Dehalococcoides* bioaugmentation cultures. In: Stroo HF, Leeson A, Ward CH, editors. Bioaugmentation for Groundwater Remediation. Springer, New York, 2013, pp. 89-115.

Sun W, Sun X, Cupples AM. Anaerobic methyl tert-butyl ether-degrading microorganisms identified in wastewater treatment plant samples by stable isotope probing. Appl Environ Microbiol 2012; 78: 2973-80.

Thelusmond JR, Strathmann TJ, Cupples AM. Carbamazepine, triclocarban and triclosan biodegradation and the phylotypes and functional genes associated with xenobiotic degradation in four agricultural soils. Sci Total Environ 2019; 657: 1138-1149.

Tusher TR, Shimizu T, Inoue C, Chien MF. Enrichment and Analysis of Stable 1,4-dioxane-Degrading Microbial Consortia Consisting of Novel Dioxane-Degraders. Microorganisms 2019; 8.

Van Hylckama VJ, De Koning W, Janssen DB. Effect of Chlorinated Ethene Conversion on Viability and Activity of *Methylosinus trichosporium* OB3b. Appl Environ Microbiol 1997; 63: 4961-4.

Wickham H. ggplot2: Elegant Graphics for Data Analysis: Springer-Verlag New York, 2016.

Xiong Y, Mason OU, Lowe A, Zhang Z, Zhou C, Chen G, et al. Investigating promising substrates for promoting 1,4-dioxane biodegradation: effects of ethane and tetrahydrofuran on microbial consortia. Biodegradation 2020; 31: 171-182.

Xiong Y, Mason OU, Lowe A, Zhou C, Chen G, Tang Y. Microbial Community Analysis Provides Insights into the Effects of Tetrahydrofuran on 1,4-Dioxane Biodegradation. Applied and Environmental Microbiology 2019; 85: e00244-19.

Yang Y, McCarty PL. Biologically Enhanced Dissolution of Tetrachloroethene DNAPL. Environmental Science & Technology 2000; 34: 2979-2984.

Yang Y, McCarty PL. Comparison between donor substrates for biologically enhanced tetrachloroethene DNAPL dissolution. Environ Sci Technol 2002; 36: 3400-4.

Ye Y, Doak TG. A parsimony approach to biological pathway reconstruction/inference for genomes and metagenomes. PLoS Comput Biol 2009; 5: e1000465.

Zenker MJ, Borden RC, Barlaz MA. Occurrence and Treatment of 1,4-Dioxane in Aqueous Environments. Environmental Engineering Science 2003; 20: 423-432.

Zhang S, Gedalanga PB, Mahendra S. Biodegradation Kinetics of 1,4-Dioxane in Chlorinated Solvent Mixtures. Environ Sci Technol 2016; 50: 9599-607.

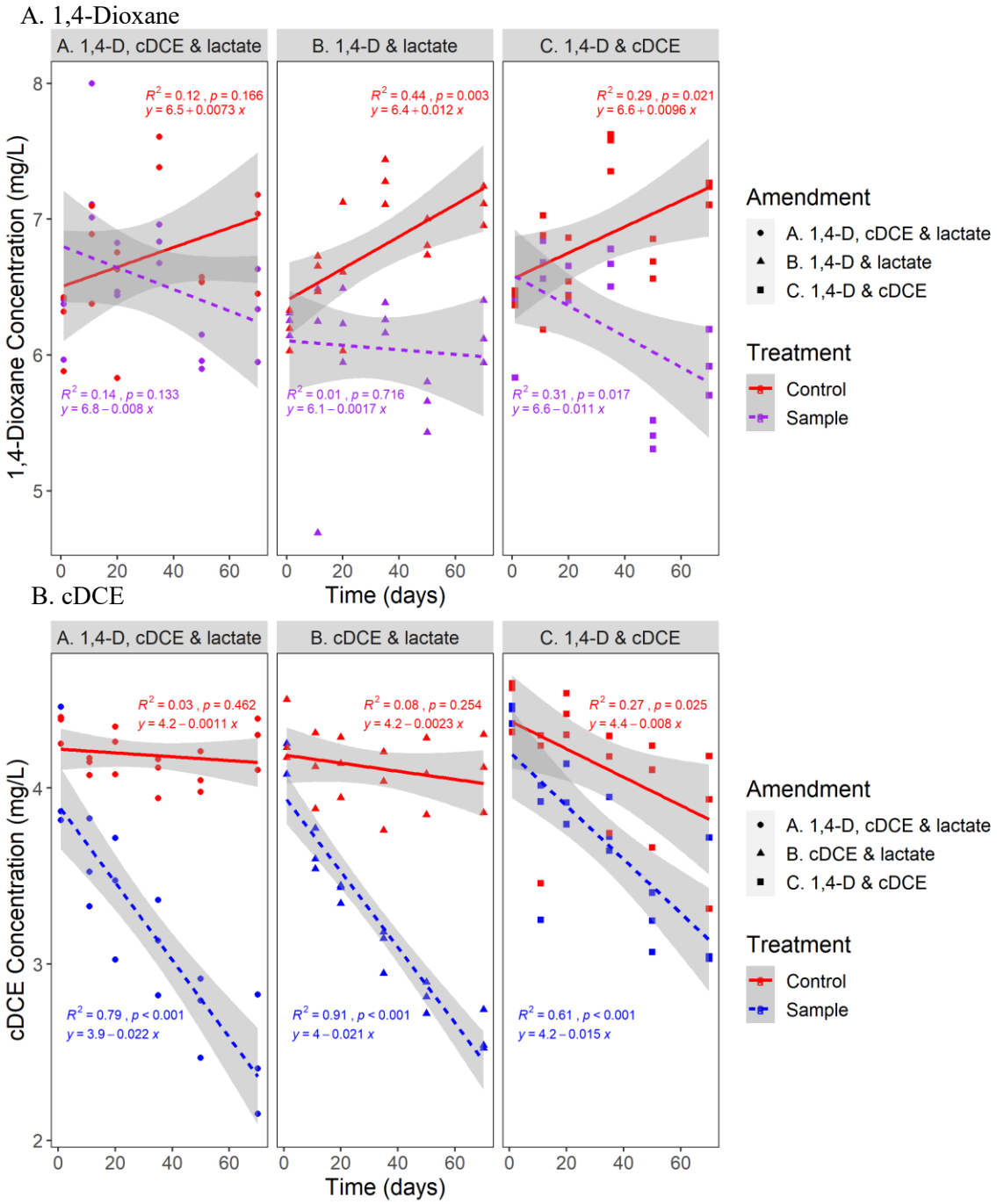

Figure 1. 1,4-Dioxane (A) and cDCE (B) concentrations in triplicate sample microcosms (purple [A] and blue [B]) and triplicate abiotic controls (red) inoculated with soil 1 and different amendments. The shaded areas indicate 95% confidence intervals along the linear regression model.

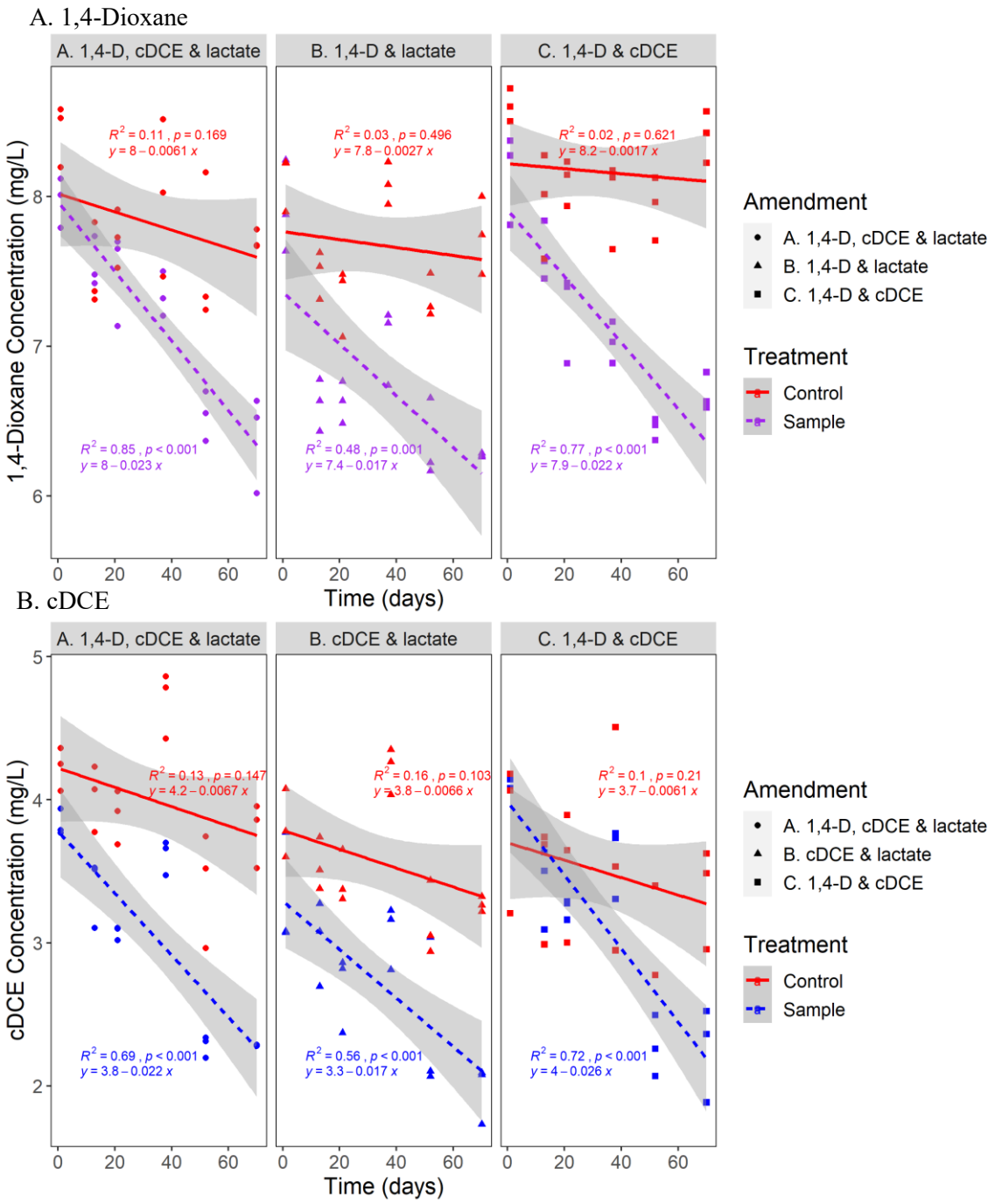

Figure 2. 1,4-Dioxane (A) and cDCE (B) concentrations in triplicate sample microcosms (purple [A] and blue [B]) and triplicate abiotic controls (red) inoculated with soil 2 and different amendments. The shaded areas indicate 95% confidence intervals along the linear regression model.

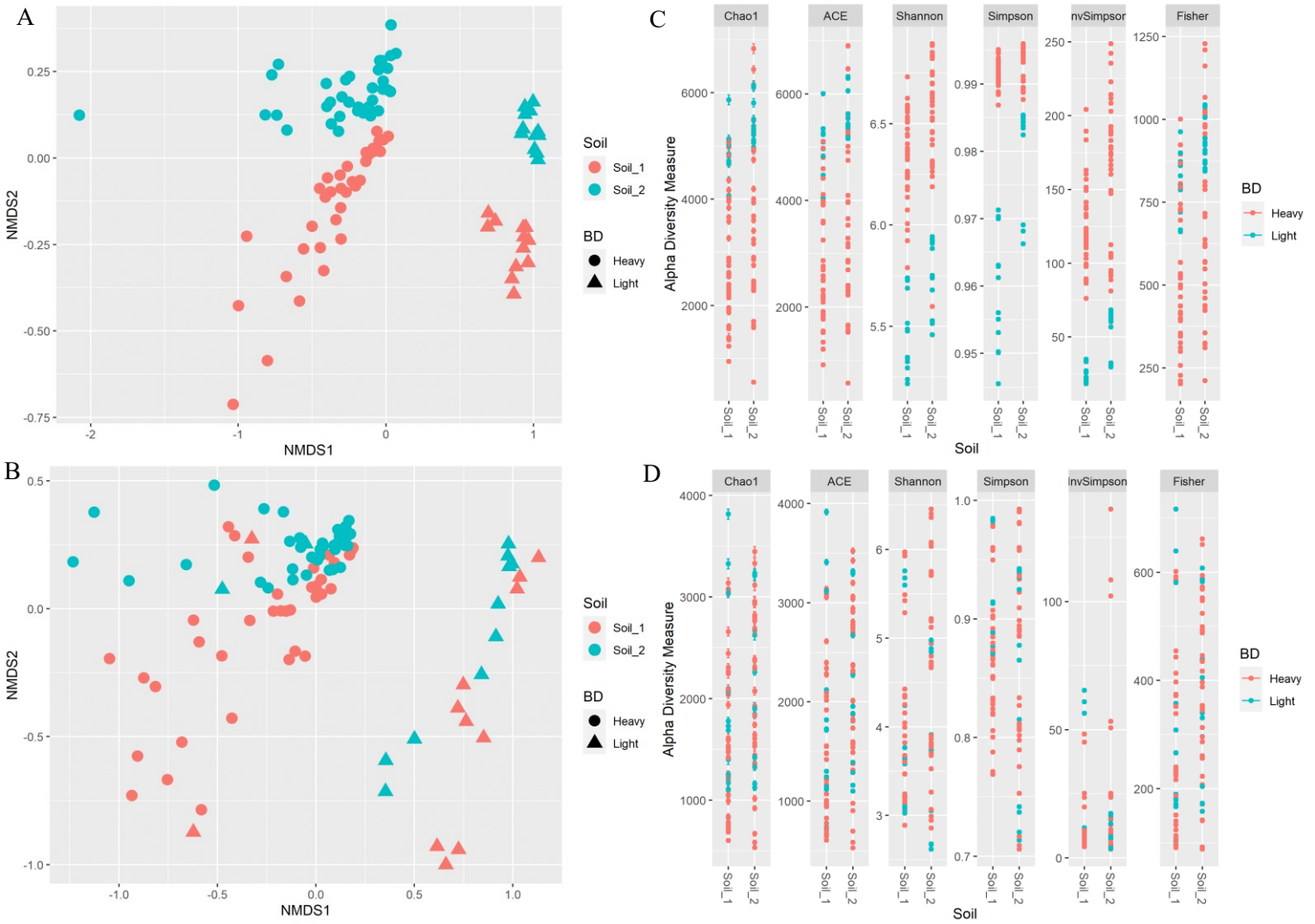

Figure 3. Non-metric Multi-Dimensional Scaling (NMDS) plots (A, B) and alpha diversity measurements (C, D) for the cDCE (A, C) and 1,4-dioxane (B, D) SIP experiments with soil 1 and 2. For each NMDS plot, for each soil, the triangles represent 12 light fractions [2 treatments (Carbon-12 or Carbon-13 amended) X 2 sample replicates × 1 light fraction × 3 sequencing replicates] and the circles represent 36 heavy fractions [2 treatments (Carbon-12 or Carbon-13 amended) X 2 sample replicates × 3 heavy fractions × 3 sequencing replicates].

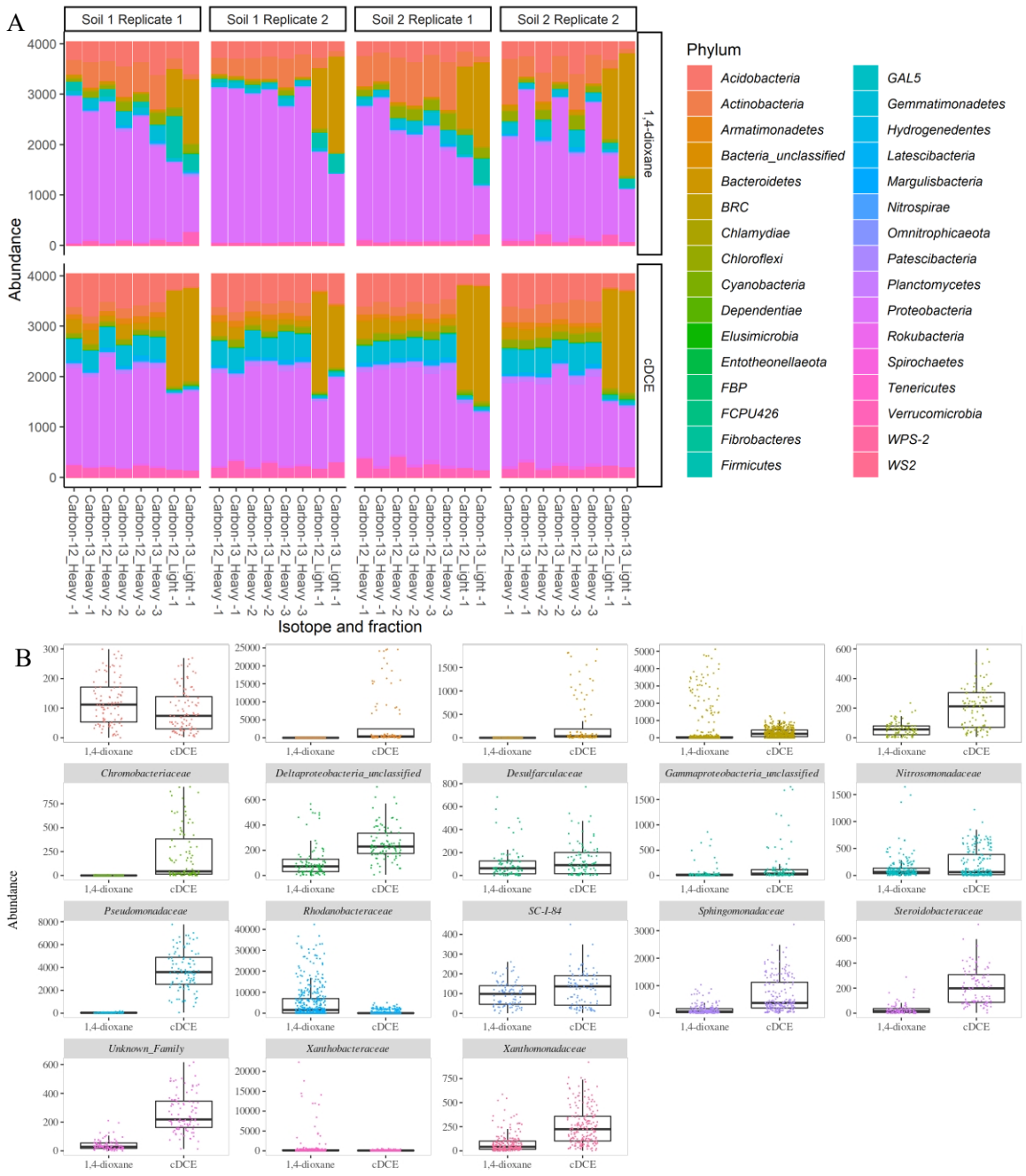

Figure 4. Classification to the phylum level for both replicates and soils amended with 1,4-dioxane (upper plot) or cDCE (lower plot) with a rarefied even depth of 95% of the minimum sum of OTU counts, each column represents cumulative values for three fractions (A). The classification (family level) of the top 30 OTUs (across all samples) within the most dominant phylum (*Proteobacteria*) (B) without rarefaction.

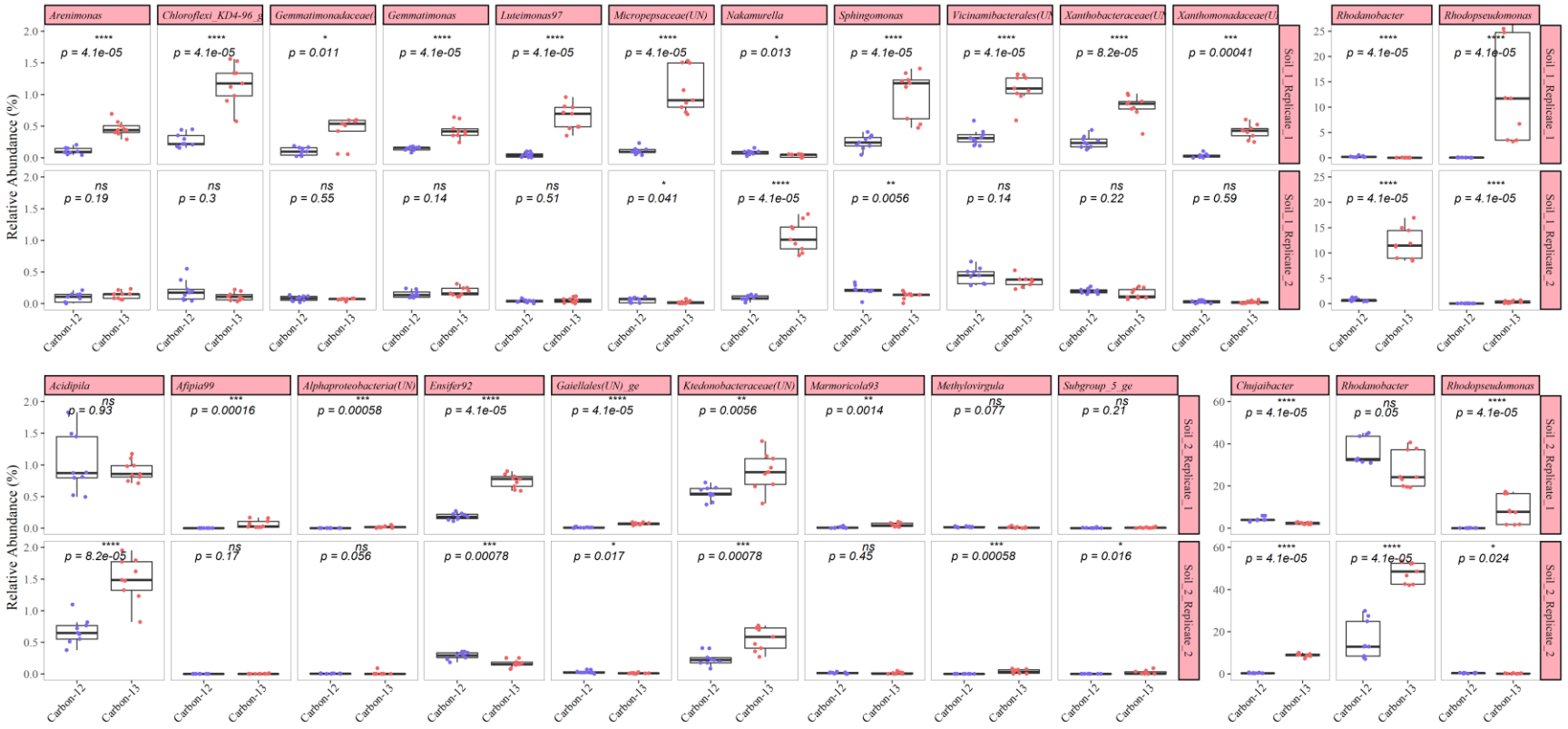

Figure 5. Boxplots with Wilcoxon Rank test results between phylotypes enriched (as determined by STAMP) in Carbon-13 amended heavy fractions (red dots) compared to the Carbon-12 amended heavy fractions (purple dots) by soil (upper is Soil 1 and lower is Soil 2) and by replicate of 1,4-dioxane amended samples. The graphs on the right have a different y-axis. P values of 0.0001, 0.001, 0.01, 0.05, >0.05 are presented by ****, ***, **, *, ns. The term "UN" denotes unclassified or uncultured microorganisms.

Figure 6. Boxplots with Wilcoxon Rank test results between phylotypes enriched (as determined by STAMP) in Carbon-13 amended heavy fractions (green dots) compared to the Carbon-12 amended heavy fractions (blue dots) by soil (upper is Soil 1 and lower is Soil 2) and by replicate of cDCE amended samples. The graphs for Soil 2 have a different y-axis. P values of 0.0001, 0.001, 0.01, 0.05, >0.05 are presented by ****, ***, **, *, ns. The term "UN" denotes unclassified or uncultured microorganisms.

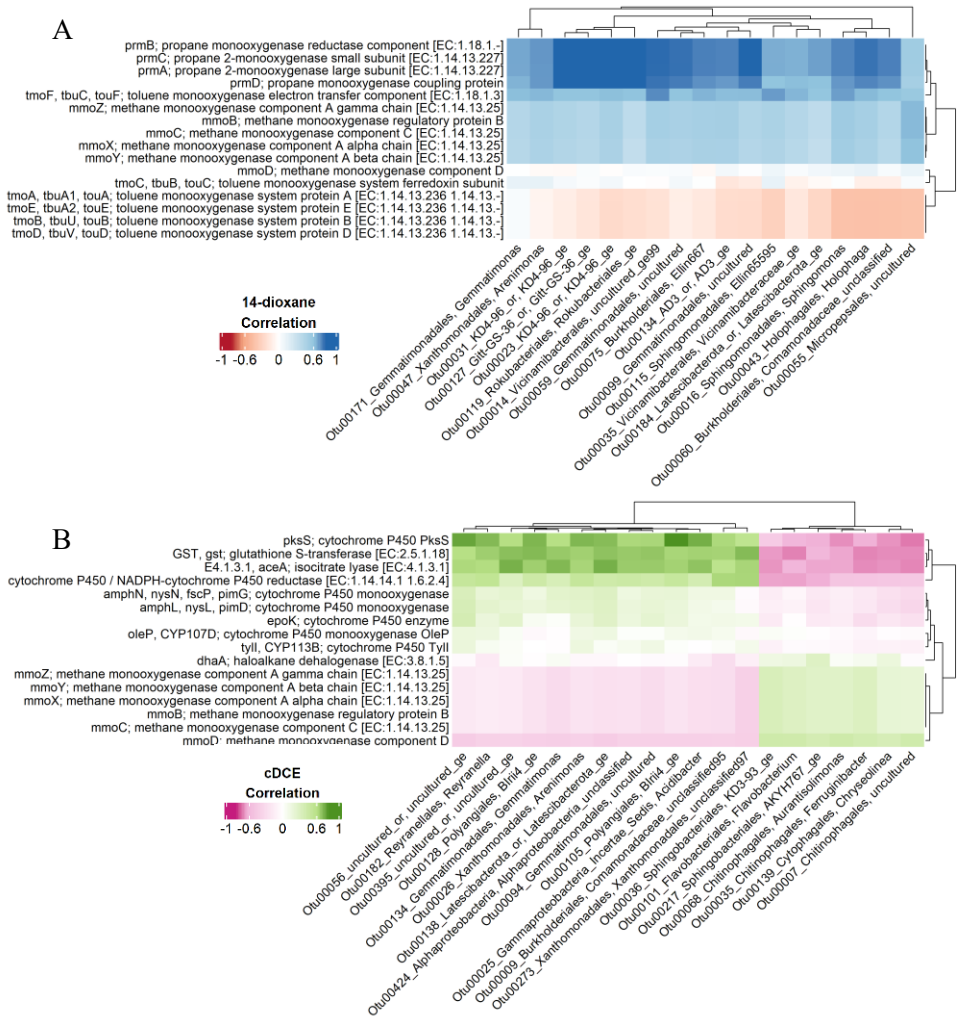

Figure 7. Correlation of KO functions associated with degradation and OTUs with average abundance higher than 0.05% from 1,4-dioxane (A) and cDCE in SIP tests. 18 OTUs had an absolute correlation coefficient high than 0.59 with at least 4 of function in 1,4-dioxane SIP. 20 OTUs had an absolute correlation coefficient high than 0.6 with at least 2 of function in 1,4-dioxane SIP.